

Physics

Physics fields

Okayama University

Year 2005

Metallic phase in the metal-intercalated
higher fullerene Rb_{8.8(7)}C₈₄

Yoshie Rikiishi, *Department of Chemistry, Okayama University*

Yoko Kashino, *Department of Chemistry, Okayama University*

Haruka Kusai, *Department of Chemistry, Okayama University*

Yasuhiro Takabayashi, *Department of Chemistry, Okayama University*

Eiji Kuwahara, *Department of Chemistry, Okayama University*

Yoshihiro Kubozono, *Department of Chemistry, Okayama University*

Takashi Kambe, *Department of Physics, Okayama University*

Taishi Takenobu, *CREST, Japan Science and Technology Agency*

Yoshihiro Iwasa, *CREST, Japan Science and Technology Agency*

Naomi Mizorogi, *Institute for Molecular Science*

Shigeru Nagase, *Institute for Molecular Science*

Susumu Okada, *Institute of Physics and Center for Computational Science, University of Tsukuba*

This paper is posted at eScholarship@OUDIR : Okayama University Digital Information Repository.

http://escholarship.lib.okayama-u.ac.jp/physics_general/34

Metallic phase in the metal-intercalated higher fullerene $\text{Rb}_{8.8(7)}\text{C}_{84}$

Yoshie Rikiishi,^{1,2} Yoko Kashino,¹ Haruka Kusai,¹ Yasuhiro Takabayashi,^{1,2} Eiji Kuwahara,^{1,2} Yoshihiro Kubozono,^{1,2,3,*} Takashi Kambe,⁴ Taishi Takenobu,^{2,5} Yoshihiro Iwasa,^{2,5} Naomi Mizorogi,⁶ Shigeru Nagase,⁶ and Susumu Okada⁷

¹Department of Chemistry, Okayama University, Okayama 700-8530, Japan

²CREST, Japan Science and Technology Agency, Kawaguchi, 332-0012, Japan

³TARA Center, University of Tsukuba, Tsukuba 305-8577, Japan

⁴Department of Physics, Okayama University, Okayama 700-8530, Japan

⁵Institute for Materials Research, Tohoku University, Sendai 980-8577, Japan

⁶Institute for Molecular Science, Okazaki 444-8585, Japan

⁷Institute of Physics and Center for Computational Science, University of Tsukuba, Tsukuba 305-8577, Japan

(Received 31 December 2004; revised manuscript received 6 April 2005; published 30 June 2005)

A new material of higher fullerene, Rb_xC_{84} , was synthesized by intercalating Rb metal into C_{84} crystals. The Rb_xC_{84} crystals showed a simple cubic (sc) structure with lattice constant, a , of 16.82(2) Å at 6.5 K, and 16.87(2) Å at 295 K. The Rietveld refinements were achieved with the space group, $Pa\bar{3}$, based on a model that the C_2 axis of $D_{2d}\text{-C}_{84}$ aligned along [111]. The sample composition was determined to be $\text{Rb}_{8.8(7)}\text{C}_{84}$. The ESR spectrum at 303 K was composed of a broad peak with peak-to-peak linewidth ΔH_{pp} of 220 G, and a narrow peak with ΔH_{pp} of 24 G. Temperature dependence of the broad peak clearly showed a metallic behavior. The metallic behavior was discussed based on a theoretical calculation. This finding of new metallic phase in a higher fullerene is the first step for a development of new types of fullerene materials with novel physical properties such as superconductivity.

DOI: 10.1103/PhysRevB.71.224118

PACS number(s): 61.48.+c, 71.20.Tx, 72.80.Rj

I. INTRODUCTION

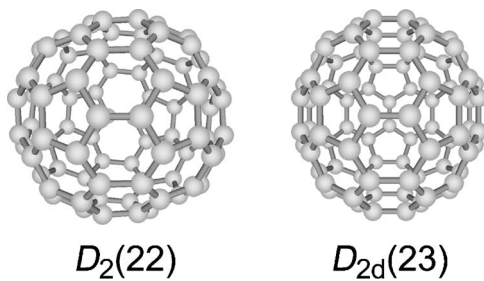
Alkaline metal intercalated C_{60} showed novel physical properties such as metallic behavior and superconductivity.¹ The highest superconducting transition temperature, T_c , was 33 K for $\text{RbCs}_2\text{C}_{60}$.² In spite of many efforts to find fullerene materials with higher T_c s, no higher T_c materials have yet been found except for Cs_3C_{60} with T_c of 40 K under 15 kbar.^{1,3} The studies on new fullerene materials have so far been limited to C_{60} and C_{70} because of difficulty in obtaining pure solid samples.¹ Recently, crystalline solid samples of metallofullerenes and higher fullerenes were obtained, and their structures have been studied by x-ray powder diffractions.^{4–8} The crystals of $M@\text{C}_{82}$ (M =lanthanide atoms) showed a cubic structure of space group $Pa\bar{3}$ [a = 15.78(1) Å for $\text{Dy}@\text{C}_{82}$, 15.78(1) Å for the C_{2v} isomer of $\text{Ce}@\text{C}_{82}$, and 15.74(4) Å for the C_s isomer of $\text{Ce}@\text{C}_{82}$].^{5–7} The photoemission (UPS),⁹ resistivity ρ ,^{5,7,8} optical spectroscopy¹⁰ and scanning tunneling spectroscopy (STS) (Ref. 11) showed a semiconductorlike behavior with small energy gap, E_g , for $M@\text{C}_{82}$ where the valence of M is +3. This result is not consistent with the theoretical prediction that $M@\text{C}_{82}$ is metallic.¹²

The crystal structures of higher fullerenes, C_{76} , C_{82} , and C_{84} , have been studied by x-ray diffraction with synchrotron radiation.^{13–15} The crystals of the toluene-solvate of C_{76} and C_{82} showed a monoclinic lattice (a = 17.68 Å, b = 11.08 Å, c = 11.02 Å, and β = 108.10° for C_{76} , and a = 18.36 Å, b = 11.36 Å, c = 11.41 Å, and β = 108.07° for C_{82}).¹³ The solvent-free crystals of C_{82} showed a simple cubic structure (sc) [space group $Pa\bar{3}$, a = 15.76(3) Å].¹⁴ The crystals of the isomer-mixture of C_{84} showed a face-centered cubic structure (fcc) at 5–295 K.¹⁵ The molecular symmetries of the

C_{84} isomers were reported to be D_2 and D_{2d} .¹⁶ Allen *et al.* first succeeded in preparing crystalline samples of metal-doped higher fullerenes by K metal intercalation into the D_2 - and $D_{2d}\text{-C}_{84}$ crystals.¹⁷ These crystals showed fcc structures with a of 16.536(6) Å for $\text{K}_{8+x}\text{C}_{84}(D_{2d})$ and 16.561(7) Å for $\text{K}_{8+x}\text{C}_{84}(D_2)$.¹⁷ Denning *et al.* reported fcc structures with a of 16.27(2) Å for $\text{K}_{3.5(1)}\text{C}_{84}(D_{2d})$ and 16.34(1) Å for $\text{K}_{2.6(1)}\text{C}_{84}(D_2)$, and suggested the metallic behavior for these crystals.¹⁸ Thus the metal-intercalated higher fullerenes have the highest potentiality towards a realization of novel physical properties among fullerenes. In the present study, we have fabricated a new metal-doped higher fullerene, Rb_xC_{84} . The crystal structure and electronic properties have been clarified by x-ray powder diffraction with synchrotron radiation and temperature dependent ESR.

II. EXPERIMENT

The C_{84} samples were prepared by an arc-discharge of graphite rods containing Eu_2O_3 . After Soxhlet-extraction of fullerenes with 1,2,4-trichlorobenzene, C_{84} was separated by a high performance liquid chromatography (HPLC) with a Buckyprep column; toluene was used as an eluent. Purified C_{84} samples were obtained by using a recycle system of HPLC. The sample purity of C_{84} was estimated to be ~99% by a time-of-flight (TOF) mass spectrometry. The C_{84} samples contained two isomers with molecular symmetries of $D_2(22)$ and $D_{2d}(23)$ where the notations in parenthesis refer to those used in Ref. 19. The molecular structures are shown in Fig. 1. These isomers are the most stable [$D_{2d}(23)$] and the second most stable [$D_2(22)$] among 24 isomers of C_{84} according to theoretical predictions.^{19,20} The abundance

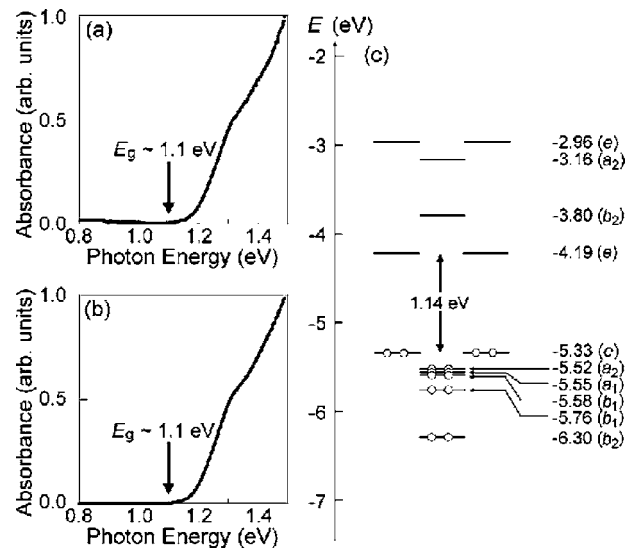
FIG. 1. Molecular structures of $D_2(22)$ - and $D_{2d}(23)$ - C_{84} .

ratio of $D_2(22)$ and $D_{2d}(23)$ isomers was estimated to be 1:4 from the HPLC profile. Solvent-free samples of C_{84} were obtained by dynamic pumping under a pressure of 10^{-5} Torr at 100 °C for 6 h, at 200 °C for 12 h and at 350 °C for 48 h. This process is similar to that for the preparation of solvent-free solids of C_{82} .¹⁴

Rb metal and the solvent-free sample of C_{84} were introduced into a glass tube in a glove box. The glass tube was sealed under a dynamic pumping at 10^{-6} Torr. The Rb_xC_{84} sample was prepared by annealing at 623 K for 618 h. The x-ray diffraction pattern for the powder sample was measured with a synchrotron radiation of $\lambda=1.0006$ Å at BL-1B of KEK-PF Tsukuba, Japan. The Rietveld refinement was carried out with the Rietan 2000 program developed by Izumi.²¹ Temperature dependent ESR spectra were measured with an X-band ESR spectrometer (Bruker ESP300) equipped with an Oxford He flow cryostat.

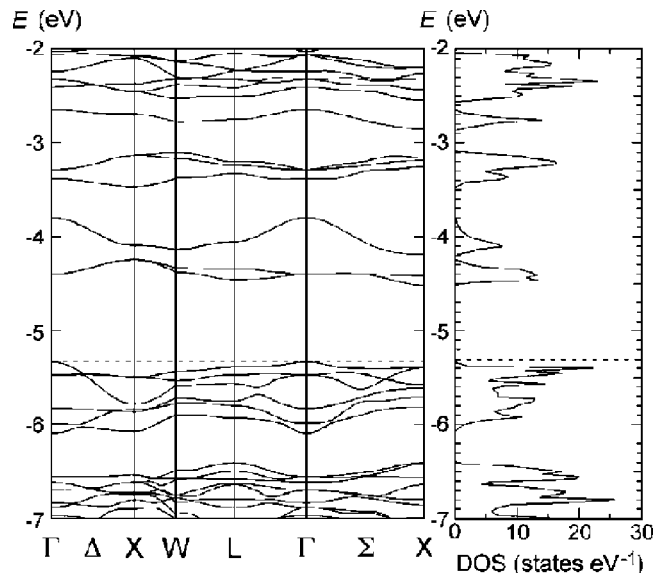
The calculation of the molecular orbital for pristine D_{2d} - C_{84} was performed using density functional theory at the BLYP/3-21G level. The electronic energy band was determined by using the local density approximation (LDA) with the norm-conserving pseudopotential and the plane-wave basis set with the cutoff energy of 50 Ry. The energy band was calculated based on the fcc structure of C_{84} which is the same as the simple cubic structure of C_{84} ($Pa\bar{3}$, $Z=4$) except for the orientation of the C_{84} cage.

The energy gap of ~ 1.1 eV opens in thin films of pristine C_{84} , as is seen from optical absorption spectra [Figs. 2(a) and 2(b)]. This value is consistent with that, 1.053 eV, estimated from the band calculation with density functional theory (DFT).²² Further, the lowest unoccupied molecular orbital (LUMO) and the highest occupied molecular orbital (HOMO) calculated for the pristine D_{2d} - C_{84} are twofold degenerate, respectively, and the HOMO-LUMO gap is 1.14 eV [Fig. 2(c)]. This value is also consistent with the optical gap of 1.1 eV. Therefore, the optical gap corresponds to the band gap of C_{84} . On the other hand, the gap energy of 0.55 eV was estimated from the plot of $\ln \rho$ versus $1/T$.²³ Recently, Shiraishi *et al.* reported that the energy gap estimated from the $\ln \rho - 1/T$ plot corresponds to the mobility gap of the thin films of C_{84} , where the mobility gap is defined as the energy difference between the actual Fermi level and the LUMO.²⁴ It should be noted that the actual Fermi level is located above the midpoint of the HOMO and the LUMO because C_{84} is an n -type semiconductor, as is suggested from the properties of the field-effect transistor (FET).²³ Actually, the energy gap of 0.55 eV observed from

FIG. 2. Optical absorption spectra of (a) mixture of $D_2(22)$ - and $D_{2d}(23)$ - C_{84} and (b) $D_{2d}(23)$ - C_{84} . (c) Molecular orbital of $D_{2d}(23)$ - C_{84} .

the plot is $\sim 1/2$ of the optical gap, i.e., the band gap. This result shows that pristine C_{84} is a normal semiconductor with small band gap of ~ 1.1 eV.

Furthermore, the band calculation for the fcc D_{2d} - C_{84} (Fig. 3) shows the existence of the narrow electronic band at -4.5 to -4.2 eV originating from a twofold degenerate e orbital, the broad band around -4 eV due to the b_2 orbital, and the narrow band at -3.5 to -3.1 eV originating from an a_2 orbital and a twofold degenerate e orbital. Therefore, the alkaline metal doping into the C_{84} crystals should produce

FIG. 3. Electronic energy band and density of states (DOS) for the fcc D_{2d} - C_{84} . Electrons are accommodated up to the dashed horizontal line. The midpoint between the LUMO and HOMO levels corresponds to the Fermi level when the C_{84} is assumed to be an intrinsic semiconductor. Actually, the exact Fermi level may be located above the midpoint because the C_{84} is an n -type semiconductor.

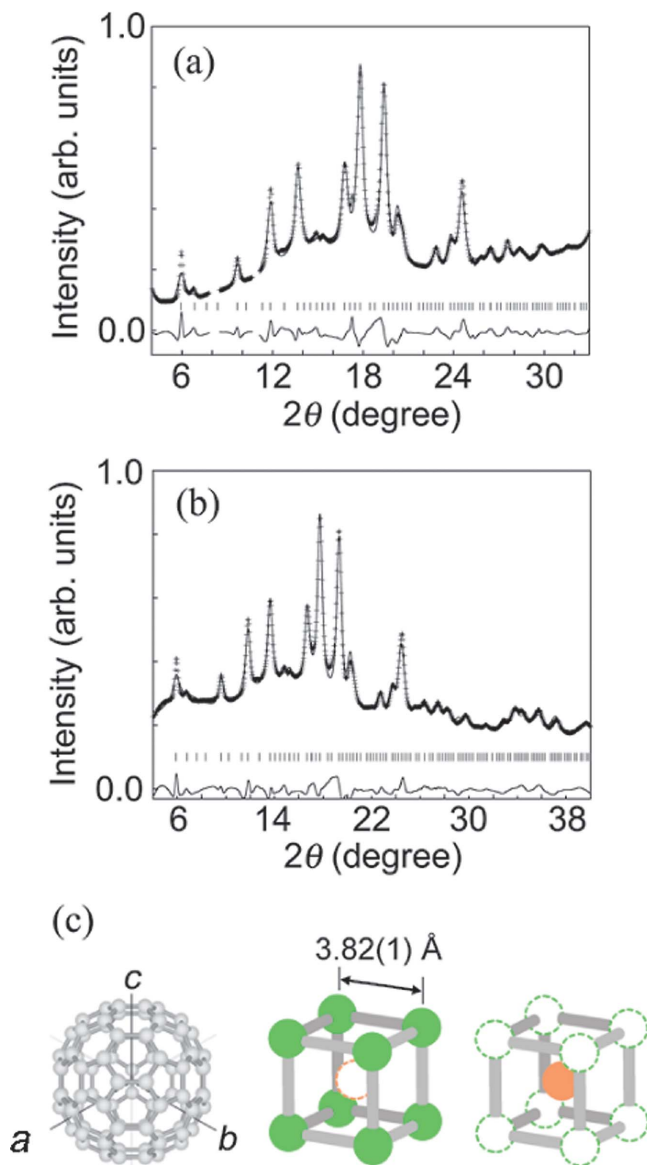


FIG. 4. (Color) X-ray diffraction patterns calculated with the structural parameters determined by Rietveld refinement (solid line) and the observed patterns (+ symbols) at (a) 6.5 and (b) 295 K. Allowed peak positions and the difference between the observed and calculated patterns are drawn by tick (middle) and solid line (bottom), respectively. (c) From left to right, $D_{2d}(23)$ - C_{84} molecule viewed along $[111]$, schematic representations of cube corners occupied by Rb and cube center occupied by Rb.

the electron-fillings for the above electronic bands.

III. RESULTS AND DISCUSSION

The x-ray diffraction patterns of $Rb_x C_{84}$ at 6.5 and 295 K are shown in Figs. 4(a) and 4(b). All Bragg reflections can be indexed as a cubic lattice with a of 16.82(2) Å at 6.5 K, and a of 16.87(2) Å at 295 K. These a values are larger by ~ 1 Å than that for the D_{2d} and D_2 isomer-mixture of C_{84} , 15.817(4) Å, at 20 K.¹⁵ Furthermore, the a of 16.87(2) Å at 295 K is larger than the values determined for $K_x C_{84}$

(16.27–16.34 Å for $K_{-3} C_{84}$, and 16.559 Å for $K_{-8} C_{84}$). The a values for $Rb_x C_{84}$ are the largest ones observed so far for the metal doped fullerenes and endohedral metallofullerenes.

In the x-ray diffraction pattern at 6.5 K, three reflections 4 3 0, 10 3 1, and 10 6 1 were observed, which do not satisfy the reflection condition for fcc ($h+k, h+l, k+l=2n$). The occurrence of 4 3 0 reflection satisfies the reflection condition, $h=2n$ for $hk0$ for the general position, $24d$, of $Pa\bar{3}$. The other space group $Pn\bar{3}$, which was a candidate of the space group in some $M@C_{82}$ crystals, requires the reflection condition, $h+k=2n$ for $hk0$.⁵ However, the occurrence of 4 3 0 reflection does not satisfy this condition. Furthermore, a trial of the Rietveld refinement with $Pm\bar{3}$, which has no reflection conditions, was not successful. Consequently, we carried out the Rietveld refinement with the space group $Pa\bar{3}$ in the same manner as $M@C_{82}$ and C_{82} .^{4–8,14} The major phase, $Rb_x C_{84}(D_{2d}(23))$, was used in the refinement. The principal C_2 axis of D_{2d} - C_{84} extends along $[111]$ [Fig. 4(c)]. The D_{2d} - C_{84} molecule must be orientationally disordered around $[111]$ to realize a cubic crystal, because the molecule has no 3 or $\bar{3}$ symmetry.

In the unit cell, the 84 C atoms occupy $24d$ position of the space group $Pa\bar{3}$ with the occupancy factor of 1/6. The Rb can occupy four sites, $(1/4, 1/4, 1/4)$, $(1/2, 1/2, 1/2)$, (x, x, x) , and $(x, x, 1-x)$. The $(1/4, 1/4, 1/4)$ and $(1/2, 1/2, 1/2)$ sites are called the tetrahedral and octahedral sites, respectively, and correspond to the $8c$ and $4b$ positions, respectively. The (x, x, x) corresponds to $8c$ position and $(x, x, 1-x)$ to $24d$ position. The C—C bond lengths in the $D_{2d}(23)$ - C_{84} were fixed at 1.36–1.47 Å. The temperature factors, B_s , of C and Rb, the occupancy factors of Rb, and x of Rb at the $8c$ and $24d$ positions were refined in the Rietveld refinement.

The calculated pattern for $Rb_x C_{84}$ at 6.5 K is shown in Fig. 4(a) together with the experimental pattern. The calculated pattern reproduces well the experimental one. The final weighted pattern R factor, R_{wp} , and integrated intensity R factor, R_I , were 4.82% and 1.31%, respectively. The refined site occupancies for the Rb atoms were 74(3)% for the tetrahedral site, 17(5)% for the octahedral site, 89(2)% for the (x, x, x) and $(x, x, 1-x)$ sites. The value of x was 0.3866(3), where the (x, x, x) and $(x, x, 1-x)$ sites constitute the cube corners of the cubes around the respective octahedral sites, as shown in Fig. 4(c). The closest Rb—Rb distance in the cube is 3.82(1) Å. This value is larger than the closest K—K distance (face-diagonal) of 3.48(2) Å in $K_{3.5(1)} C_{84}$ (Ref. 18) and that (cube-edge) of 3.631(2) Å in $K_{8.39(17)} C_{84}$.¹⁷ This result reflects larger ionic radius of Rb than K. The closest Rb—Rb refers to cube edge sites as in $K_{8.39(17)} C_{84}$ but does not refer to face-diagonal sites;^{17,18} the corners of the cube are almost completely occupied by Rb atoms in the present phase. When the center of the cube is occupied by Rb, the closest Rb—Rb (center-corner) distance should be 3.31 Å. It is too small in comparison with the distance expected from the ionic radius of Rb. Therefore, the corner sites [green balls in Fig. 4(c)] can be expected to be vacant when the cube center is occupied by Rb [orange ball in Fig. 4(c)], and con-

TABLE I. Structural parameters of Rb in $\text{Rb}_{8.8(7)}\text{C}_{84}$.

x	y	z	B (\AA^2)	Fractional occupancy (%)
		6.5 K		
1/4	1/4	1/4	11(2)	74(3)
1/2	1/2	1/2	27(15)	17(5)
0.3866(3)	0.3866(3)	0.3866(3)	2(2)	89(2)
0.3866(3)	0.3866(3)	0.6134(3)	13(2)	89(2)
		295 K		
1/4	1/4	1/4	9(1)	70(2)
1/2	1/2	1/2	22(15)	13(4)
0.3867(3)	0.3867(3)	0.3867(3)	9(5)	87(2)
0.3867(3)	0.3867(3)	0.6133(3)	11(2)	87(2)

versely the cube center should be vacant when the corner sites are occupied. If this is the case, the site occupancies of cube-corner and cube-center should be 8/9 ($\sim 89\%$) and 1/9 ($\sim 11\%$), respectively, whose values are consistent with the site occupancies, 89(2)% for the cube corner $[(x,x,x)$ and $(x,x,1-x)]$ and 17(5)% for the cube center $[(1/2,1/2,1/2)]$, determined by this Rietveld refinement.

From the Rietveld refinement, the x is determined to be 8.8(7) for Rb_xC_{84} . Similar phase was found in K-intercalated C_{84} , i.e., $\text{K}_{8.39(17)}\text{C}_{84}$ and $\text{K}_{8.86(1)}\text{C}_{84}$. The phase of $\text{A}_{8.8(7)}\text{C}_{84}$ may be formed selectively because of the occupancies of 8/9 at (x,x,x) and $(x,x,1-x)$ and that of 1/9 at $(1/2,1/2,1/2)$ which are reasonable occupancies to prevent the Rb metal occupying both cube-center and cube-corners. These facts suggest that such stoichiometry corresponds to one of the stable phases in alkaline-metal doped C_{84} crystals.

The B s were $1(2)\text{\AA}^2$ for C, $11(2)\text{\AA}^2$ for Rb at $(1/4,1/4,1/4)$, $27(15)\text{\AA}^2$ for Rb at $(1/2,1/2,1/2)$, $2(2)\text{\AA}^2$ for Rb at $(0.3866,0.3866,0.3866)$, and $13(2)\text{\AA}^2$ for Rb at $(0.3866,0.3866,0.6134)$. The B of C is close to that of K_3C_{60} , $1.2(5)\text{\AA}^2$.²⁵ The large B of Rb at the $(1/2,1/2,1/2)$ site originates from larger spatial site than the $(1/4,1/4,1/4)$ site, as in the case of K_3C_{60} .²⁵ The Rietveld refinement by assuming coexistence of two phases of $\text{Rb}_x\text{C}_{84}(D_{2d})$ and $\text{Rb}_x\text{C}_{84}(D_2)$ was also tried, but further improvements were not obtained. In the Rietveld refinement with the space group $P2_13$, which is a maximal subgroup of $P\bar{a}3$, the B of C fell into negative value. Thus a possibility of the $P2_13$ was rejected.

The Rietveld refinement was performed for the x-ray diffraction pattern at 295 K based on the structure at 6.5 K. The calculated pattern is shown in Fig. 4(b) together with the experimental one. The final R_{wp} and R_1 were 3.66% and 1.73%, respectively. The site occupancies of Rb were 70(2)% at $(1/4,1/4,1/4)$, 13(4)% at $(1/2,1/2,1/2)$, 87(2)% at (x,x,x) and $(x,x,1-x)$ sites. The composition can be estimated to be $\text{Rb}_{8.4(5)}\text{C}_{84}$. It is consistent with that, $\text{Rb}_{8.8(7)}\text{C}_{84}$, at 6.5 K within the standard uncertainty, and each site occupancy is also consistent with that at 6.5 K. This result shows that the occupancies determined by the Rietveld

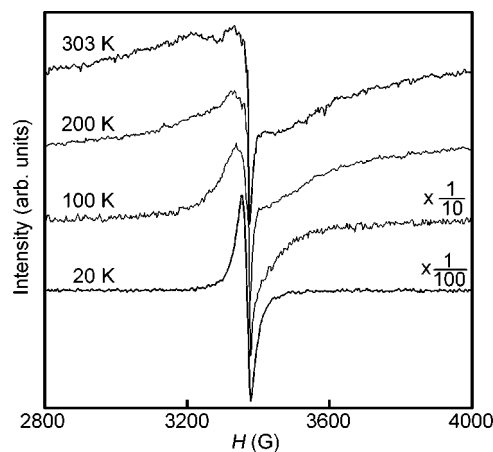
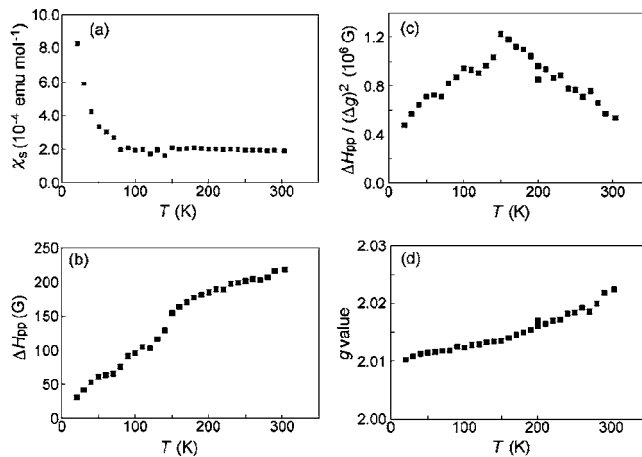


FIG. 5. Temperature-dependent ESR spectra at 20, 100, 200, and 303 K.

refinement are reliable. In the subsequent part of this paper we adopt $\text{Rb}_{8.8(7)}\text{C}_{84}$ determined at 6.5 K as the composition of the sample. The B of C increased from $1(2)\text{\AA}^2$ at 6.5 K to $3(1)\text{\AA}^2$ at 295 K. The B s of Rb were almost constant even when the temperature was changed from 6.5 to 295 K, which shows that the B s of Rb are substantially defined by a static disorder. Structural parameters of Rb are listed in Table I.

Temperature-dependent ESR spectra for $\text{Rb}_{8.8(7)}\text{C}_{84}$ are shown in Fig. 5. The ESR spectrum at 303 K is composed of at least two peaks, and the spectrum was analyzed with two Lorentz peaks. The peak-to-peak linewidth, ΔH_{pp} , for the broad peak is 220 G. The ΔH_{pp} is smaller than that for Rb_3C_{60} , 490 G,²⁶ while it is much larger than the values for K_xC_{84} [~ 4 G for $\text{K}_{2.6(1)}\text{C}_{84}(D_{2d})$, ~ 6 G for $\text{K}_{3.5(1)}\text{C}_{84}(D_{2d})$, and 3.5 G for $\text{K}_{8.86(11)}\text{C}_{84}(D_{2d}+D_2)$].^{17,18} The ΔH_{pp} for the narrow peak is 24 G at 303 K. The broad spectrum becomes narrower with decreasing temperature (Fig. 5). The temperature dependence of spin susceptibility, χ_s , estimated from the broad peak is shown in Fig. 6(a). The χ_s shows a constant value down to 80 K, suggesting a Pauli-type χ_s . The intensity of the narrow peak increased drastically at low tempera-

FIG. 6. Temperature dependence of (a) χ_s , (b) ΔH_{pp} , (c) $\Delta H_{pp}/(\Delta g)^2$, and (d) g .

ture, showing a Curie-type behavior and a small Curie constant of 1.4×10^{-3} emu K mol $^{-1}$; the ΔH_{pp} of the narrow peak was constant at 20–303 K. Thus it was difficult to extract the exact intensity of the broad peak owing to an existence of the intense narrow peak at low temperature. Therefore the intensity of the broad peak increased apparently at low temperature, due to the narrow peak ascribed to the defect spin. Thus the intensity of the broad peak is expected to be constant even below 80 K.

The ΔH_{pp} estimated from the broad peak linearly increases with an increase in temperature [Fig. 6(b)]. This result shows that the phase of $\text{Rb}_{8.8(7)}\text{C}_{84}$ is metallic. The temperature dependence of ΔH_{pp} for $\text{Rb}_{8.8(7)}\text{C}_{84}$ is consistent with those for $\text{K}_{3.5(1)}\text{C}_{84}$ and $\text{K}_{2.7(1)}\text{C}_{84}$ which are concluded to be metallic.¹⁸ Elliot showed that ΔH_{pp} was related to the g shift, Δg , relative to the g value, 2.0023, of the free electron as $\Delta H_{pp} \sim (\Delta g)^2 / \tau$ when the dominant contribution to spin-lattice relaxation rate was the modulation of spin-orbit interactions by phonon; τ is relaxation time in the Drude model.^{27,28} The ΔH_{pp} of three-dimensional (3D) conventional metals follows the above expression. Here it should be noted that the $\Delta H_{pp} / (\Delta g)^2$ is proportional to ρ in the 3D metals. The plot of $\Delta H_{pp} / (\Delta g)^2$ versus T is shown in Fig. 6(c). The $\Delta H_{pp} / (\Delta g)^2$ value increases linearly with increasing temperature up to 150 K, showing clearly metallic behavior. A drastic change is observed around 150 K in this plot. Above 150 K the $\Delta H_{pp} / (\Delta g)^2$ value decreases monotonically up to 300 K. Such a change was not observed in plots of χ_s and ΔH_{pp} versus T [Figs. 6(a) and 6(b)]. On the other hand, a linear relationship was found in the $\Delta H_{pp} / (\Delta g)^2$ plots in Rb_3C_{60} , K_3C_{60} , and $\text{Na}_2\text{CsC}_{60}$ which are recognized to be metallic.²⁶ The drastic change in the plot of $\Delta H_{pp} / (\Delta g)^2$ versus T is caused by a rapid increase in g value above 150 K [Fig. 6(d)]. Such a rapid increase in g was observed in $\text{Cs}_{3.3(1)}\text{C}_{60}$.²⁹ The variation of temperature dependence of g and $\Delta H_{pp} / (\Delta g)^2$ may imply the presence of a structural phase transition or change of molecular motion, because the g value is sensitive to structural variation around the conduction electron. However, no structural phase transitions were observed in C_{84} below 300 K.¹⁵ This fact does not actively support the presence of the structural phase transition in $\text{Rb}_{8.8(7)}\text{C}_{84}$. Thus the temperature dependent-ESR suggests that $\text{Rb}_{8.8(7)}\text{C}_{84}$ is metallic, but the origin of the variation of temperature dependence of g and $\Delta H_{pp} / (\Delta g)^2$ remains to be clarified.

The MO calculation for the pristine $D_{2d}(23)\text{-C}_{84}$ shown in Fig. 2(c) suggests that the twofold degenerate e orbital at -2.96 eV is singly occupied in $\text{Rb}_{8.8(7)}\text{C}_{84}$ because of ~ 9 electron-transfer from Rb to C_{84} . The theoretical density of states (DOS) for fcc $D_{2d}\text{-C}_{84}$ calculated for the band at -3.3 to -3.1 eV is close to that for the band at -4.5 to -4.2 eV, as seen from Fig. 3. The band at -3.3 to -3.1 eV corresponds to the twofold degenerate e orbital and the band is partial-filled in $\text{Rb}_{8.8(7)}\text{C}_{84}$. The narrow electronic band at -4.5 to -4.2 eV should be partial-filled in $\text{K}_{3.5(1)}\text{C}_{84}$ and $\text{K}_{2.7(1)}\text{C}_{84}$. The theoretical calculation (Fig. 3) predicts that

the DOS on the Fermi level, $D(\epsilon_F)$, for $\text{Rb}_{8.8(7)}\text{C}_{84}$ is close to those for $\text{K}_{3.5(1)}\text{C}_{84}$ and $\text{K}_{2.7(1)}\text{C}_{84}$, if the doping causes no significant modification of the energy band.

The broad ESR peak (Fig. 5) could be assigned to the conduction electron ESR (c -ESR); the broad spectrum was analyzed with Lorentz line shape. It should be noted that the c -ESR spectrum does not show a Dysonian line shape because this sample is fine crystals. The χ_s of $\text{Rb}_{8.8(7)}\text{C}_{84}$ estimated from the broad peak at 303 K was 1.9×10^{-4} emu mol $^{-1}$ which corresponds to the Pauli susceptibility. The $D(\epsilon_F)$ was estimated to be 2.9 states eV $^{-1}$ C_{84}^{-1} spin $^{-1}$ from the χ_s . This value is close to those for $\text{K}_{3.5(1)}\text{C}_{84}$ (2.01 states eV $^{-1}$ C_{84}^{-1} spin $^{-1}$) and $\text{K}_{2.7(1)}\text{C}_{84}$ (2.63 states eV $^{-1}$ C_{84}^{-1} spin $^{-1}$),¹⁸ as is expected from the theoretical calculation (Fig. 3). The slight increase in $D(\epsilon_F)$ of $\text{Rb}_{8.8(7)}\text{C}_{84}$ in comparison to those for $\text{K}_{3.5(1)}\text{C}_{84}$ and $\text{K}_{2.7(1)}\text{C}_{84}$ is probably due to the lattice expansion from ~ 16.3 Å to 16.87(2) Å.

The synthesis of the fullerene material, $\text{Rb}_{8.8(7)}\text{C}_{84}$, with the largest a among metal doped fullerenes and endohedral metallofullerenes was of significance for a realization of superconductors based on fullerenes other than C_{60} , because the large $D(\epsilon_F)$ is expected owing to the small transfer integral between the fullerene molecules. However, the $D(\epsilon_F)$ value of $\text{Rb}_{8.8(7)}\text{C}_{84}$, 2.9 states eV $^{-1}$ C_{84}^{-1} spin $^{-1}$, is smaller than those of K_3C_{60} (14 states eV $^{-1}$ C_{60}^{-1} spin $^{-1}$), Rb_3C_{60} (19 states eV $^{-1}$ C_{60}^{-1} spin $^{-1}$), and Cs_3C_{60} (9 states eV $^{-1}$ C_{60}^{-1} spin $^{-1}$).^{30,31} The small $D(\epsilon_F)$ of $\text{Rb}_{8.8(7)}\text{C}_{84}$ may not lead to a significant T_c in the BCS model, and the superconducting transition could not be observed down to 2 K. Furthermore, the structural disorder that two isomers of $D_{2(22)}$ and $D_{2d}(23)\text{-C}_{84}$ are contained in this sample may be responsible for no observation of superconductivity in $\text{Rb}_{8.8(7)}\text{C}_{84}$. In fact it is suggested that the existence of two phases, body-centered orthorhombic and cubic, destroys the superconductivity in Cs_3C_{60} under ambient pressure.^{3,29} Thus, the structural disorder will not produce a positive effect for an appearance of superconductivity. Nevertheless, the finding of a new metallic phase in metal doped higher fullerene is very important for the development of new carbon-cluster materials with novel physical properties.

The χ_s due to defect spin, 3.6×10^{-6} emu mol $^{-1}$, estimated from the narrow peak of the ESR at 303 K is smaller by two orders of magnitudes than the χ_s ascribable to Pauli susceptibility, 1.9×10^{-4} emu mol $^{-1}$. The Curie constant for the χ_s due to the defect spin results in a very small unpaired electron, 4×10^{-3} spin per C_{84} , whose value is smaller than those of K_xC_{84} , 0.1–0.3 per C_{84} .^{17,18} This implies that the $\text{Rb}_{8.8(7)}\text{C}_{84}$ sample has less defects than K_xC_{84} . Recently, it was found that $M@\text{C}_{82}$ is not metallic but semiconductor-like, regardless of the fact that odd numbers of electrons are transferred to the C_{82} cage from the encapsulated metal atom.^{5–11} However, the metallic behavior found in $\text{Rb}_{8.8(7)}\text{C}_{84}$ can be explained by the simple band picture, as in the case of alkaline metal doped C_{60} .¹ This indicates the possibility of materials design with higher fullerenes conducted by theoretical calculation.

ACKNOWLEDGMENTS

The authors acknowledge Professor Mototada Kobayashi of University of Hyogo for his valuable suggestion in x-ray diffraction measurements, and Miss Rie Watanabe of Okayama University for her kind assistance in sample preparation. The x-ray diffraction study was performed under the

proposal of KEK-PF, 2002G201. This work was supported by a Grant-in-Aid (15350089) from the Ministry of Education, Culture, Sports, Science and Technology of Japan, by Okayama University COE Project, by the Mitsubishi Foundation, and by the Visiting Researcher's program Institute for Materials Research of Tohoku University (2003).

*Electronic mail: kubozone@cc.okayama-u.ac.jp

- ¹Y. Iwasa and Y. Takenobu, *J. Phys.: Condens. Matter* **15**, R495 (2003).
- ²K. Tanigaki, T. W. Ebbesen, S. Saito, J. Mizuki, J. S. Tsai, Y. Kubo, and S. Kuroshima, *Nature (London)* **352**, 222 (1991).
- ³T. T. M. Palstra, O. Zhou, Y. Iwasa, P. E. Sulewski, R. M. Fleming, and B. R. Zegarski, *Solid State Commun.* **93**, 327 (1995).
- ⁴Y. Takabayashi, Y. Kubozono, T. Kanbara, S. Fujiki, K. Shibata, Y. Haruyama, T. Hosokawa, Y. Rikiishi, and S. Kashino, *Phys. Rev. B* **65**, 073405 (2002).
- ⁵Y. Kubozono, Y. Takabayashi, K. Shibata, T. Kanbara, S. Fujiki, S. Kashino, A. Fujiwara, and S. Emura, *Phys. Rev. B* **67**, 115410 (2003).
- ⁶K. Shibata, Y. Rikiishi, T. Hosokawa, Y. Haruyama, Y. Kubozono, S. Kashino, T. Uruga, A. Fujiwara, H. Kitagawa, T. Takano, and Y. Iwasa, *Phys. Rev. B* **68**, 094104 (2003).
- ⁷Y. Rikiishi, Y. Kubozono, T. Hosokawa, K. Shibata, Y. Haruyama, Y. Takabayashi, A. Fujiwara, S. Kobayashi, S. Mori, and Y. Iwasa, *J. Phys. Chem. B* **108**, 7580 (2004).
- ⁸T. Hosokawa, S. Fujiki, E. Kuwahara, Y. Kubozono, H. Kitagawa, A. Fujiwara, T. Takenobu, and Y. Iwasa, *Chem. Phys. Lett.* **395**, 78 (2004).
- ⁹S. Hino, H. Takahashi, K. Iwasaki, K. Matusmoto, T. Miyazaki, S. Hasegawa, K. Kikuchi, and Y. Achiba, *Phys. Rev. Lett.* **71**, 4261 (1993).
- ¹⁰C. J. Nuttall, Y. Hayashi, K. Yamazaki, T. Mitani, and Y. Iwasa, *Adv. Mater. (Weinheim, Ger.)* **14**, 293 (2002).
- ¹¹S. Fujiki, Y. Kubozono, Y. Rikiishi, and T. Urisu, *Phys. Rev. B* **70**, 235421 (2004).
- ¹²S. Amamiya, S. Okada, S. Suzuki, and K. Nakao, *Synth. Met.* **121**, 1137 (2001).
- ¹³H. Kawada, Y. Fujii, H. Nakao, Y. Murakami, T. Watanuki, H. Suematsu, K. Kikuchi, Y. Achiba, and I. Ikemoto, *Phys. Rev. B* **51**, 8723 (1995).
- ¹⁴Y. Kubozono, Y. Rikiishi, K. Shibata, T. Hosokawa, S. Fujiki, and H. Kitagawa, *Phys. Rev. B* **69**, 165412 (2004).
- ¹⁵S. Margadonna, C. M. Brown, T. J. S. Dennis, A. Lappas, P. Pattison, K. Prassides, and H. Shinohara, *Chem. Mater.* **10**, 1742 (1998).
- ¹⁶T. J. S. Dennis, T. Kai, T. Tomiyama, and H. Shinohara, *Chem. Commun. (Cambridge)* **1998**, 619.
- ¹⁷K. M. Allen, T. J. S. Dennis, M. J. Rosseinsky, and H. Shinohara, *J. Am. Chem. Soc.* **120**, 6681 (1998).
- ¹⁸M. S. Denning, T. J. S. Dennis, M. J. Rosseinsky, and H. Shinohara, *Chem. Mater.* **13**, 4753 (2001).
- ¹⁹P. W. Fowler and D. E. Manolopoulos, *An Atlas of Fullerenes* (Clarendon, Oxford, 1995).
- ²⁰K. Kobayashi, and S. Nagase, in *Endofullerenes: A New Family of Carbon Clusters*, edited by T. Akasaka and S. Nagase (Kluwer Academic, Dordrecht, 2002), p. 99.
- ²¹F. Izumi, in *The Rietveld Method*, edited by R. A. Young (Oxford University Press, Oxford, 1993), p. 236.
- ²²S. Saito, S. Sawada, N. Hamada, and A. Oshiyama, *Jpn. J. Appl. Phys., Part 1* **32**, 1438 (1993).
- ²³K. Shibata, Y. Kubozono, T. Kanbara, T. Hosokawa, A. Fujiwara, Y. Ito, and H. Shinohara, *Appl. Phys. Lett.* **84**, 2572 (2004).
- ²⁴M. Shiraishi, K. Shibata, R. Maruyama, and M. Ata, *Phys. Rev. B* **68**, 235414 (2003).
- ²⁵P. W. Stephens, L. Mihaly, P. L. Lee, R. L. Whetten, S.-M. Huang, R. Kaner, F. Deiderich, and K. Holczer, *Nature (London)* **351**, 632 (1991).
- ²⁶P. Petit, J. Robert, T. Yildirim, and J. E. Fischer, *Phys. Rev. B* **54**, R3764 (1996).
- ²⁷R. J. Elliott, *Phys. Rev.* **96**, 266 (1954).
- ²⁸L. Alcacer, in *Organic Conductors, Fundamentals and Applications*, edited by J.-P. Farges (Marcel Dekker, New York, 1994), p. 269.
- ²⁹S. Fujiki, Y. Kubozono, M. Kobayashi, T. Kambe, Y. Rikiishi, S. Kashino, K. Ishii, H. Suematsu, and A. Fujiwara, *Phys. Rev. B* **65**, 235425 (2002).
- ³⁰A. P. Ramirez, *Supercond. Rev.* **1**, 1 (1994).
- ³¹Y. Kubozono, S. Fujiki, K. Hiraoka, T. Urakawa, Y. Takabayashi, S. Kashino, Y. Iwasa, T. Kitagawa, and Y. Mitani, *Chem. Phys. Lett.* **298**, 335 (1998).